View metadata, citation and similar papers at core.ac.uk
brought to you by CORE
provided by Elsevier - Publisher Connector

Biophysical Journal Volume 96 March 2009 2335–2343

The Effects of ADF/Cofilin and Profilin on the Conformation of the ATP-Binding Cleft of Monomeric Actin

Roland Kardos,[†] Kinga Pozsonyi,[†] Elisa Nevalainen,[‡] Pekka Lappalainen,[‡] Miklós Nyitrai,[†] and Gábor Hild[†]*
[†]University of Pécs, Faculty of Medicine, Department of Biophysics, Pécs, Hungary; and [‡]University of Helsinki, Institute of Biotechnology, Program in Cell and Molecular Biology, Helsinki, Finland

ABSTRACT Actin depolymerizing factor (ADF)/cofilin and profilin are small actin-binding proteins, which have central roles in cytoskeletal dynamics in all eukaryotes. When bound to an actin monomer, ADF/cofilins inhibit the nucleotide exchange, whereas most profilins accelerate the nucleotide exchange on actin monomers. In this study the effects of ADF/cofilin and profilin on the accessibility of the actin monomer's ATP-binding pocket was investigated by a fluorescence spectroscopic method. The fluorescence of the actin bound ε-ATP was quenched with a neutral quencher (acrylamide) in steady-state and time dependent experiments, and the data were analyzed with a complex form of the Stern-Volmer equation. The experiments revealed that in the presence of ADF/cofilin the accessibility of the bound ε-ATP decreased, indicating a closed and more compact ATP-binding pocket induced by the binding of ADF/cofilin. In the presence of profilin the accessibility of the bound ε-ATP increased, indicating a more open and approachable protein matrix around the ATP-binding pocket. The results of the fluorescence quenching experiments support a structural mechanism regarding the regulation of the nucleotide exchange on actin monomers by ADF/cofilin and profilin.

INTRODUCTION

The structure and dynamics of the actin cytoskeleton are regulated by a large number of proteins that interact with monomeric and/or filamentous actin (1,2). Among the central regulators of cytoskeletal dynamics in all eukaryotes are ADF/cofilin and profilin.

Actin depolymerizing factor (ADF)/cofilins are small actin-binding proteins (molecular mass = 15–19 kDa) that can bind monomeric and filamentous actin as well (3–5). In cells, ADF/cofilins promote the disassembly of aged actin filaments, and thus play an essential role in cytoskeletal dynamics in organisms from yeasts to mammals (6,7). ADF/cofilins were shown to increase the monomer dissociation rate at the filaments' pointed ends from 0.35 s^{-1} to 9 s^{-1} (8) and to promote filament severing (9). ADF/cofilins preferentially bind and disassemble ADP-actin filaments (8,10). Most ADF/cofilins also bind ADP-G-actin (K_d = 0.02–0.15 μM) with significantly higher affinity than ATP-G-actin (K_d = 0.2–8 μM) (8,11,12). When bounding to an actin monomer they inhibit the rate of nucleotide exchange (8,9,13–15).

ADF/cofilins compete with other actin-binding proteins (e.g., profilin, gelsolin segment 1) in actin binding, which suggests that they bind to the hydrophobic cleft between the subdomains 1 and 3 of actin (16–19). This was recently confirmed by determining the structure of twinfilin's actin depolymerizing factor homology domain (ADF-H) in complex with actin (20). Twinfilin is an evolutionarily conserved protein that interacts with actin through its two ADF-H domains, which are structurally and functionally homologous to the single ADF-H domain of ADF/cofilins (21–24). This crystal structure suggest that binding of the ADF-H domain of ADF/cofilin or twinfilin to the hydrophobic cleft between actin subdomains 1 and 3 may ''lock'' the cleft between subdomains 2 and 4 in a closed conformation. The hydrophobic cleft is located close to a region containing α-helices that bridges the two major domains of the actin (Q137-S145; P333-S338) and are probably responsible for the relative motion of the main domains (25). The connection of the ABPs to the hydrophobic cleft may have an allosteric effect on the α-helices region, which can be involved in the control of the opening and closing state of the nucleotide binding cleft (26).

Differential scanning calorimetry studies showed that the binding of ADF/cofilin to actin shifted the melting point of the G-actin from 62.8°C to 68.0°C, which indicates a strong stabilizing effect on the G-actin structure (27). Radiolytic oxidative protein footprinting experiments showed that residues located at the top of the nucleotide-binding cleft in the subdomain 4, within the cleft and also in the subdomain 2 were protected against oxidation in the actin-cofilin binary complex (28). Based on these observations it was suggested that the binding of cofilin to G-actin caused the closure of the actin's nucleotide binding pocket. Furthermore, Muhlrad et al. (29) showed that cofilin can inhibit the accessibility of the fluorescent nucleotide in filamentous actin.

Profilins are small actin binding proteins (molecular mass = ~19 kDa) (30) distributed diffusely in the cytoplasm and expressed in great extent in the eukaryotic cells (31). Contrary to ADF/cofilin, profilins bind exclusively to the monomeric form of actin, and prefer the ATP bound form of it (32–36).

The main function of profilin is to increase the dynamics of the pool of monomeric actin in the cytoplasm (2). Profilins

Submitted September 22, 2008, and accepted for publication December 8, 2008.

*Correspondence: gabor.hild@aok.pte.hu

Editor: Cristobal G. dos Remedios.

© 2009 by the Biophysical Society

0006-3495/09/03/2335/9 $2.00

doi: 10.1016/j.bpj.2008.12.3906

promote the incorporation of the ATP-actin monomers into the filament at the barbed ends, and through interactions with poly-proline stretches profilins feed actin monomers to formins and VASP family proteins (35,37–39). Most profilins also enhance the nucleotide exchange on actin monomers (40–43) and profilin is also able to compensate the inhibiting effect of ADF/cofilin on the nucleotide dissociation from the G-actin (16). The function of the profilin is controlled by phosphoinositides (e.g., PIP_2) via preventing the formation of the actin-profilin complex (44).

Crystal structures of many profilin isoforms have been determined by x-ray diffraction and NMR methods (33, 45–47). The actin-profilin atomic structure shows that the profilin binds to an area between the subdomains 1 and 3 on the actin monomer (20,26,48,49). This binding appears to cause the opening of the nucleotide-binding cleft due to the relative movement of the two main domains (26,48,49). Computational calculations suggested that the opening of the nucleotide-binding pocket might occur via shear motions involving the α-helical region connecting the two major domains (41,50). Molecular dynamic simulations showed that the nucleotide binding cleft closed within 200 ps after removing the profilin from the actin-profilin complex because of the thermodynamic instability of the actin in the absence of the profilin (50). A conformational shift around the nucleotide binding region was also emphasized in connection with other monomer binding proteins (51–53). Thymosin-β_4 was considered to bind the subdomain 2 and decrease the nucleotide exchange on actin due to stabilizing the nucleotide binding cleft in a closed conformational state (51,52). Other results showed that the binding of the thymosin-β_4 between the subdomain 2 and 4 locks the actin in a dynamically restricted structural state (53). In all these studies the structure of the nucleotide binding cleft was considered to be important for understanding the detailed function of the different monomer binding regulatory proteins.

Despite the crystallographic data and modeling experiment, the possible effects of ADF/cofilin and profilin on the conformation of actin monomer in solution have not been reported previously. In this study we carried out fluorescence quenching experiments on G-actin labeled with a fluorescent ATP analog (ε-ATP) in the presence and absence of ADF/cofilin and profilin to investigate the conformational and/or dynamic changes in the protein matrix around the fluorophore. The results showed that ADF/cofilin and profilin had antagonistic effect. The accessibility of the fluorophore decreased in the presence of the ADF/cofilin, whereas in the presence of the profilin it increased. These findings correlate with the property of cofilin and profilin altering the nucleotide exchange on G-actin observed previously. Therefore, in the case of the profilin the nucleotide-binding pocket of actin is in a more open state (the fluorophore is more accessible to the quencher), which can facilitate the nucleotide exchange. On the contrary, ADF/cofilin inhibits the quenching of the fluorophore, which indicates a more compact nucleotide-binding pocket. This closing pocket may result in a decrease in the nucleotide exchange rate on G-actin.

MATERIALS AND METHODS

Reagents

KCl, $CaCl_2$, TRIS (tris-(hydroxy-methyl)amino-methane), $MgCl_2$, acrylamide, and DOWEX 1×2-400 were purchased from Sigma-Aldrich (Budapest, Hungary). ATP, MEA (mercaptoethanol), and NaN_3 were supplied by Merck (Budapest, Hungary). The ε-ATP (etheno-ATP) was obtained from the Invitrogen (Carlsbad, CA).

Protein preparation

Acetone-dried muscle powder was obtained from rabbit skeletal muscle as was described earlier by Feuer et al. (54). The calcium bound G-actin was prepared according to the method of Spudich and Watt modified by Mossakowska et al. (55,56). The G-actin was stored in buffer A, containing 4 mM Tris-HCl, 0.2 mM ATP, 0.1 mM $CaCl_2$, 0.5 mM MEA, and 0.005% NaN_3 at pH 8.0. The concentration of the G-actin was determined spectrophotometrically with a Shimadzu UV-2100 spectrophotometer by using the absorption coefficient of 1.11 mg ml^{-1} cm^{-1} at 280 nm (57). The relative molecular mass of 42,300 Da was used for G-actin (58).

Yeast cofilin and profilin were expressed as glutathione S-transferase (GST) and His-tagged fusion proteins, respectively. The plasmid constructions were transformed into *Escherichia coli* BL21 cells. The cells were grown in 5000 mL Luria broth medium at 37°C until the optical density of the sample got 0.7 at 600 nm. The protein expression was induced by 0.3 mM isopropyl-β-D-thiogalactopyranoside (IPTG) and the cells were harvested overnight at 20°C.

The cells producing recombinant cofilin molecules were dissolved in an extraction buffer containing 50 mM TRIS-HCl, 5 mM DTE, 50 mM NaCl, 5 mM EDTA, 10% glycerol and 1 mM PMSF at pH 7.6. The cells were lysed by homogenization and sonication and the suspension was centrifuged for 30 min at 30,000 × g.

The cofilin-GST fusion proteins were removed from the supernatant by using a column with glutathione-agarose beads. The GST beads bound recombinant cofilin molecules were incubated overnight with thrombin to separate the cofilin from GST. The glutathione-agarose column was connected to a Sephacryl S-300 column to separate the cofilin from any contaminating components. The peak fractions of cofilin eluted from the column was pooled and concentrated in a 10 kDa cutoff Amicon Ultracentrifugal filter device (Millipore, Billerica, MA) to a final concentration of 300–400 μM.

The cells producing His-tagged profilin were resuspended in extraction buffer (50 mM TRIS, 10 mM Imidazole, 250 mM NaCl at pH 7.5) and lysed by homogenization and sonication. The suspension was centrifuged for 30 min at 30,000 × g. The supernatant was loaded onto a nickel-nitrilotriacetic acid-agarose column and eluted with a buffer containing 250 mM imidazole (250 mM imidazole, 50 mM NaCl, 10 mM TRIS at pH 7.5). The elution fluid was loaded onto a Sephacryl S-300 gel filtration column to separate the profilin from contaminating factors. The peak fractions of profilin was collected and concentrated in a 10 kDa cutoff Amicon Ultracentrifugal filter device (Millipore) to a final concentration of 300–400 μM. The concentration of cofilin and profilin was calculated at 280 nm with a Shimadzu UV-2100 spectrophotometer by using an absorption coefficient of 1.002 mg ml^{-1} cm^{-1} and 1.458 mg ml^{-1} cm^{-1}, respectively (estimated based on amino acid composition by ProtParam; http://us.expasy.org/tools).

Preparation of the ε-ATP bound actin monomers

A fluorescent nucleotide analog (ε-ATP) was attached to the Ca-G-actin according to the method of Perelroizen et al. (42). Ion exchanger resin (180 μl; 50% DOWEX 1×2-400) was added to 50 μM G-actin in 1.2 mL A-buffer to remove the unbound ATP from the solution. The mixture of

the G-actin and the ion exchanger resin was immediately centrifuged (13,200 $\times$ g on 4°C for 3 min) to avoid the dissociation of the bound ATP from the actin molecules. The supernatant was mixed again with the same amount of DOWEX-1 to ensure that only a negligible fraction of free ATP remained in the solution. The centrifugation step was repeated to clarify the G-actin solution from the ion exchanger resin completely. The sample of Ca-G-actin (50 μM) was mixed with a fivefold molar excess of ε-ATP (final concentration, 250 μM) and was kept on ice overnight. The next day 1 mL ε-ATP-actin was treated with 0.1 mL 50% DOWEX 1×2-400 resin for short time (few seconds) to decrease the amount of the free ε-ATP in the solution. The actin concentration was determined spectrophotometrically by using the absorption coefficient of 1.11 mg ml^{-1} cm^{-1} at 280 nm (57).

Fluorescence quenching experiments

Steady-state fluorescence measurements were carried out with a Perkin-Elmer (Waltham, MA) LS50B and a Horiba Jobin Yvon (Longjumeau, France) Fluorolog-3 spectrofluorometer equipped with a thermostable cuvette holder. The ε-ATP-actin (5 μM) in ATP free buffer A solution was titrated with a neutral quencher (acrylamide). The concentration of the quencher was increased from 0 to 0.3 M in the solution. The excitation wavelength was set at 320 nm and the emission spectrums were recorded between 330 nm and 600 nm with 5 nm slits on the excitation and emission side as well. The experiments were carried out at 20°C. Time-resolved Fluorescence measurements were carried out with an ISS K2 Multifrequency Phase Fluorometer (ISS Fluorescence Instrumentation, Champaign, IL). The applied quencher concentration was within the range of 0 and 0.3 M in the cuvette. Freshly prepared glycogen solution was used as a reference with a lifetime of 0 ns. The phase delay and demodulation ratio of the sample fluorescence signal was measured in respect to the phase delay and demodulation ratio of the reference. The source of the excitation light was a 300 W Xe arc lamp. The intensity of the light was modulated sinusoidally by a double-crystal Pockel cell. The excitation wavelength was set at 320 nm and the emitted light was monitored through an FG 385 high-pass filter. The modulation frequency was varied in 10 steps from 2 to 64 MHz. The data were analyzed by the "Vinci version BETA.1.6" software. The fluorescence lifetime of the ε-ATP was calculated by using nonlinear least-square analysis. The goodness of fit was estimated from the value of the reduced χ^2 probe (59). Fig. 1 shows the change of the phase delay and the modulation ratio of the sinusoidally modified fluorescence emission signal in the case of the ε-ATP labeled actin monomers (Fig. 1).

Data analysis

One way to analyze the data collected in steady-state measurements is by using the classical Stern-Volmer equation (60):

$$\frac{F_0}{F} = 1 + K_{SV}[Q], \tag{1}$$

where the F_0 is the fluorescence intensity of the sample in the absence of the quencher molecule whereas F is the fluorescence intensity at different quencher concentration [Q]. The Stern-Volmer quenching constant (K_{SV}) is the sum of the static and dynamic quenching processes that can be described by the static (K_{SV_S}) and dynamic (K_{SV_D}) quenching constants and can be related to the accessibility of the fluorophore to the quencher molecules.

The data obtained by time dependent measurements can also be approached by using the Stern-Volmer equation (60):

$$\frac{\tau_0}{\tau} = 1 + K_{SV\_D}[Q] = 1 + k_q\tau_0[Q], \tag{2}$$

where the τ_0 is the fluorescence lifetime of the fluorophore in the absence of the quencher, whereas τ is the lifetime at different quencher concentration. The K_{SV_D} is the dynamic Stern-Volmer constant, which is the product of the dynamic rate constant (k_q) and the lifetime of the fluorophore measured in the absence of the quencher molecules (τ_0).

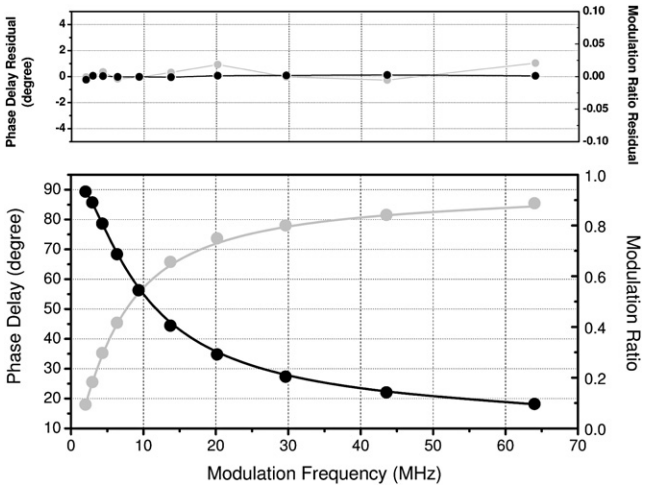

FIGURE 1 Frequency domain measurement of the ε-ATP labeled actin monomers. (*Upper panel*) The difference between the measured data values and the fits (residuals) were plotted for the phase delay (*solid symbols*) and modulation ratio (*shaded symbols*) at different modulation frequencies. (*Lower panel*) The change of the phase delay (*solid symbols*) and the modulation ratio (*shaded symbols*) of the signal form ε-ATP labeled actin monomers was recorded in a frequency range between 2 and 64 MHz in the absence of acrylamide.

A special situation when the static and dynamic quenching processes are both affecting the fluorescence signal can be handled by the following equation (60):

$$\frac{F_0}{F} = (1 + K_{SV\_S}[Q])(1 + K_{SV\_D}[Q]). \tag{3}$$

In a complex situation, when both static and dynamic quenching processes are responsible for the decrease of the fluorescence intensity and more than one fluorophore population can be found in the sample with different accessibility the following equation can be used:

$$\frac{F_0}{F} = \left(\sum_{i=1}^{n} \frac{f_i}{(1 + K_{SV\_Si}[Q])(1 + K_{SV\_Di}[Q])}\right)^{-1} \tag{4}$$

where K_{SV_Si} and K_{SV_Di} are the static and dynamic Stern-Volmer constant of the ith population represented by the fraction of f_i, respectively.

RESULTS AND DISCUSSION

In spectroscopic studies etheno-nucleotides are used widely to explore the molecular details behind the function of different intracellular proteins (61–64). In this study, we carried out steady-state and time-resolved fluorescence quenching measurements with acrylamide to explore the change in the protein matrix around the ε-ATP placed in the nucleotide-binding pocket in the presence of cofilin and profilin.

Quenching of the free ε-ATP

The effectiveness of the quenching of the steady-state fluorescence from the free ε-ATP was determined in the presence of 5 μM ε-ATP dissolved in buffer A at 20°C. The acrylamide concentration was changed from 0 to 0.3 M. The

analysis of the data showed that the K_{SV} value was 53.6 ± 3.19 M^{-1} ($n = 3$) for the free ε-ATP that is similar to previous results (61,64).

Fluorescence lifetime measurements were also carried out with 50 μM ε-ATP at 20°C in the presence of different acrylamide concentration (0–0.3 M). The initial value of the identified single lifetime decreased from 24.52 ± 0.01 ns ($\chi^2 = 2.41$; $n = 3$) to 1.41 ± 0.03 ns ($\chi^2 = 2.63$; $n = 3$) in the presence of 0.3 M acrylamide. Previous results also showed a single lifetime component (27 ns) for the free ε-ATP that could be effectively quenched by collisional processes (62). The analysis of the results showed that the dynamic quenching constant is 54.05 ± 1.02 M^{-1} ($n = 3$) that is nearly identical to the value (53.6 M^{-1}) that was calculated in the case of the steady-state measurements.

As the quenching constants from these different measurements are practically the same we concluded that the fluorescence of the free ε-ATP was only quenched by dynamic but not static quenching processes. This conclusion confirms the former results of Harvey and Cheung (62).

Quenching of the actin-bound ε-ATP

The steady-state quenching experiments with actin bound ε-ATP were completed in the presence of 5 μM actin. The acrylamide effectively decreased the fluorescence intensity of the fluorophore at the applied quencher concentrations (0–0.3M) (Fig. 2 *A*). The classical Stern-Volmer plots (Eq. 1) from the steady-state measurements showed a downward curvature. At different ε-ATP concentrations data points ended at different levels due to the variable ratios of bound and unbound ε-ATP (Fig. 2 *B*).

We carried out time dependent fluorescence measurements on the ε-ATP labeled actin monomers to evaluate the role of dynamic quenching processes related to the bound fraction of the ε-ATP in the nonlinear relationship between the F_0/F and the quencher concentration (Q). In these measurements the actin concentration was in the range of 20–30 μM. In the absence of the quencher it was possible to identify two distinct lifetime components with the values of 34.1 ± 4.5 ns and 25.4 ± 0.1 ns (Fig. 3 *A*). The latter was very close to what we obtained in the absence of actin. Based on the values of these lifetime components we attributed these lifetimes to the fractions of the actin bound and free ε-ATP.

Harvey and Cheung (62) found that the lifetime of the G-actin bound ε-ATP was 36 ns. They successfully quenched the free ε-ATP with acrylamide but the fluorescence of the monomeric actin bound ε-ATP was not affected by collisional quenching processes. The longer lifetime component we observed (34.1 ns) was independent of the acrylamide concentration (Fig. 3 *A*, *upper panel*), which is similar to their results.

The shorter lifetime component decreased from 25.4 ± 0.1 ns to 1.55 ± 0.05 ns as the acrylamide concentration increased from 0 to 0.3 M (Fig. 3 *A*, *lower panel*). The slope

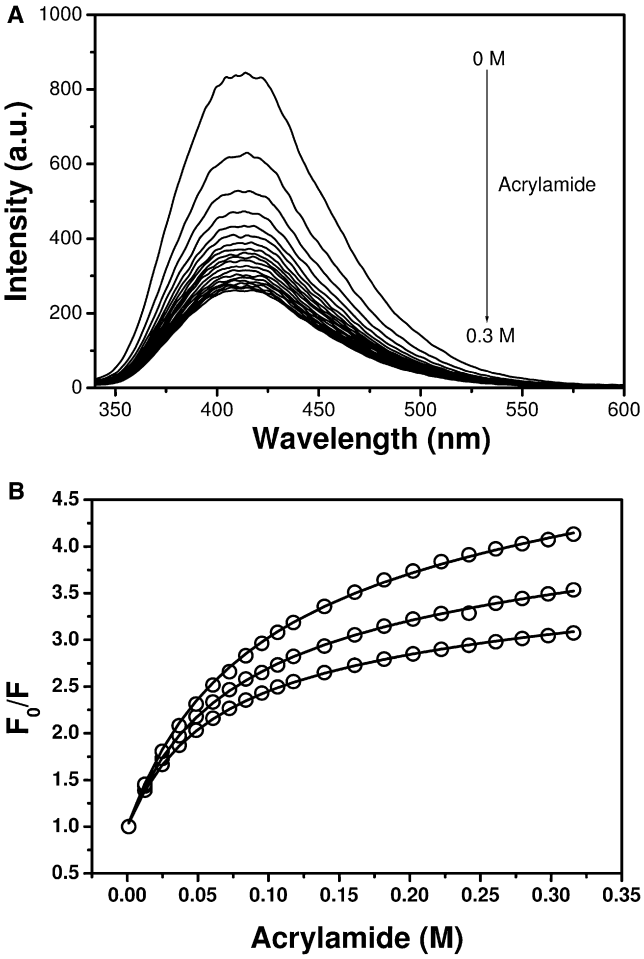

FIGURE 2 Results from the steady-state quenching measurements with ε-ATP labeled actin monomers. (*A*) The change of the fluorescence spectrum of the ε-ATP labeled monomers (5 μM) in the presence of increasing acrylamide concentration (0–0.3 M). (*B*) The Stern-Volmer plot of three independent steady-state quenching experiments with the actin-bound ε-ATP (5 μM actin) in the presence of different acrylamide concentrations (0–0.3M). Solid lines represents the fits obtained with the Eq. 4. The calculated K_{SV_S} value is 0.24 ± 0.05 M^{-1} for the actin bound ε-ATP molecules.

of the Stern-Volmer plot for this component was 49.20 ± 4.28 M^{-1} (Fig. 3 *B*), which is similar to the value we obtained for the free ε-ATP molecules (54.05 ± 1.02 M^{-1}). The correlation with previous results and between the data we obtained in the absence and presence of actin corroborated that this lifetime component belonged to the free ε-ATP.

The complex situation behind the downward curved Stern-Volmer plots of the steady-state measurements can be treated by using Eq. 4. This equation can be used to obtain detailed information about the fluorescence of the actin-bound ε-ATP.

K_{SV_D} for the free ε-ATP was 54.05 ± 1.02 M^{-1}, whereas the value of K_{SV_S} was negligible. K_{SV_D} for the monomeric actin bound ε-ATP also proved to be negligible so the only unknown parameters in this equation are the fractional component (f) and K_{SV_S} for the bound fluorophore. By

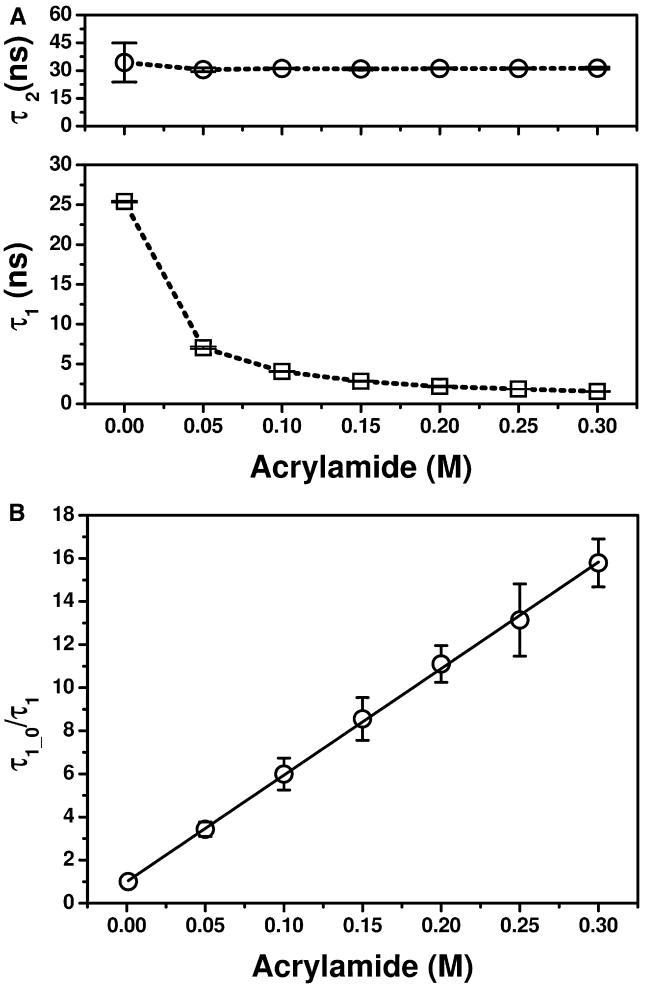

FIGURE 3 Quenching of the fluorescence lifetime of ε-ATP labeled actin monomers with acrylamide. (*A*) The upper panel shows the longer lifetime component (τ_2) that belongs to the actin bound ε-ATP whereas the lower panel shows the quenching of the shorter lifetime (τ_1) of the free ε-ATP. (*B*) The Stern-Volmer plot of the shorter lifetime of the free ε-ATP (τ_1) in the presence of different acrylamide concentrations (0–0.3M). The solid line represents the fit of the Eq. 2 to the obtained experimental data. The value for the K_{SV_D} was 49.20 ± 4.28 M^{-1} for the free ε-ATP in the solution. The error bars represent the values of SD.

using the known values as fixed components and the unknowns as variables it was possible to evaluate the measured data points with the complex Stern-Volmer equation (Eq. 4).

Although the fractional contributions of the unbound and bound components were usually different in the samples the static quenching constant could be determined confidently with this analysis. K_{SV_S} value for the actin bound ε-ATP was 0.24 ± 0.05 M^{-1} whereas the fraction of the free ε-ATP varied in the range of 70–79%. The calculated K_{SV_S} value was two orders of magnitude smaller than the K_{SV_D} of the free ε-ATP. This finding is in good agreement with theoretical considerations suggesting that the quenching of the fluorescent labels can decrease with 2 orders of magnitude due to the binding to a protein. In this case the decrease of the quenching efficiency can occur due to the shielding of the fluorescent dye by the surrounding protein matrix (65).

The described complex behavior of the protein bound ε-ATP is not unique as a similar behavior of ε-ATP was seen before with myosin by Rosenfeld and Taylor (64). The results of their steady-state quenching experiments showed similar downward tendency on the classic Stern-Volmer plots. They concluded that the presence of the free ε-ATP and the protein bound ε-ATP together with their different accessibility to the different quenching processes could cause the downward curvature of the plots from the steady-state measurements (64). Similar explanation is reasonable for our observations.

Based on our measurements we conclude that the actin bound ε-ATP cannot be quenched through dynamic quenching processes and the static component of its quenching can be represented by a K_{SV_S} value of 0.24 ± 0.05 M^{-1}.

Quenching of the actin-bound ε-ATP in the presence of actin-binding proteins

The fluorescence quenching experiment with the ε-ATP bound monomeric actin was repeated in the presence of cofilin. During the steady-state experiments the concentration of cofilin was 15 μM whereas the actin concentration was 5 μM. The acrylamide concentration was varied from 0 to 0.3 M (Fig. 4 *A*). Considering that the affinity of the applied cofilin for the ATP-actin monomers is 0.59 μM (12) the unbound fraction of the actin was ~5% (~0.3 μM). The presence of this small fraction in the solution was considered negligible during the analysis of the data. The Stern-Volmer plot of the data showed downward curvature with a floating endpoint (Fig. 4 *B*) similar to what was observed in the absence of the actin-binding protein (Fig. 2 *B*).

To evaluate the nonlinearity of the plotted data points we carried out time dependent fluorescence quenching experiments with the ε-ATP bound actin monomers in the presence of cofilin. In this case we increased the actin concentration to 10 μM to get a useful amount of fluorescence signal during the lifetime measurements. To keep the fraction of the actin that is not bound to cofilin on a negligible level (<2%) we increased the cofilin concentration to 20 μM. The time dependent fluorescence measurements identified two ε-ATP populations with two distinct lifetime components. The shorter lifetime component changed from 25.82 ± 0.85 ns (τ_1) to 1.52 ± 0.85 ns as the acrylamide concentration raised to 0.3 M. The calculated K_{SV_D} value from the Stern-Volmer plot of this fluorescence lifetime component was 48.02 ± 8.35 M^{-1}. The value of this long lifetime component and the calculated K_{SV_D} also suggested that this component belonged to the free ε-ATP population in the sample.

The longer lifetime component (τ_2) was 30.4 ns and it practically did not change whereas the acrylamide reached its final 0.3 M concentration. The value of this component

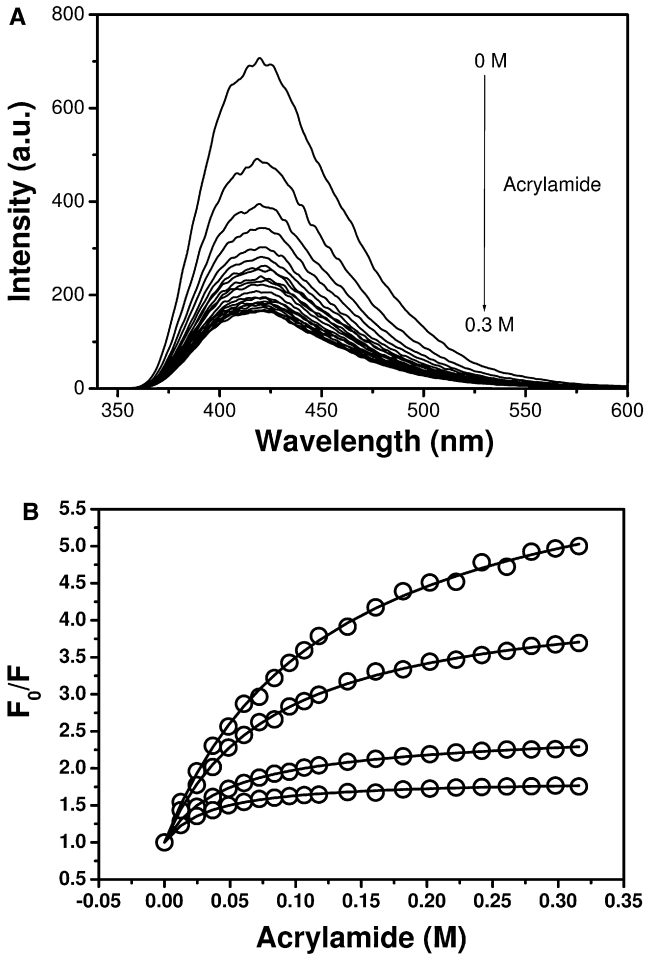

FIGURE 4 Quenching of the fluorescence of ε-ATP labeled actin monomers with acrylamide in the presence of ADF/cofilin molecules. (*A*) The change of the fluorescence spectrum of the ε-ATP labeled monomers (5 μM) in the presence of ADF/cofilin (15 μM) with increasing acrylamide concentration (0–0.3 M). (*B*) The Stern-Volmer plots from the steady-state quenching experiments with 5 μM ε-ATP labeled actin monomers in the presence of 15 μM cofilin (○) at different acrylamide concentrations (0–0.3 M). The calculated K_{SV_S} value was $0.034 \pm 0.017\ M^{-1}$ for the actin bound ε-ATP in the presence of cofilin.

and its constant level suggested that this lifetime component belonged to the actin bound ε-ATP as it was the case in the absence of the actin-binding protein as well. These data suggest that the effect of dynamic quenching processes on the fluorescence of the actin bound ε-ATP is negligible in the presence of cofilin.

Considering the results of the time dependent fluorescence measurements and the data defined for the free ε-ATP the Eq. 4 can be used to determine the K_{SV_S} value for the fluorescent nucleotide. The other unknown parameter is the ratio of the unbound ε-ATP that usually varied between different preparations.

When the data from the steady-state measurements were fitted with the Eq. 4 the previously identified parameters ($K_{SV\_S\_free-\varepsilon ATP}$, $K_{SV\_D\_free-\varepsilon ATP}$, $K_{SV\_D\_bound-\varepsilon ATP}$) were used as fixed components whereas $K_{SV\_S\_bound-\varepsilon ATP}$ and f_i were considered as variables. From this fitting procedure $K_{SV\_S\_bound-\varepsilon ATP}$ for the ε-ATP bound to the actin monomers in complex with the cofilin can provide valuable information about the structural change induced by the actin binding protein around the bound nucleotide.

In the presence of cofilin the value of the static quenching constant (K_{SV_S}) for the actin bound ε-ATP was $0.034 \pm 0.017\ M^{-1}$ (Fig. 4 *B*) and the fraction of the free ε-ATP was in the range of 46–85% ($n = 4$). These results show that K_{SV_S} was approximately a factor of 7 smaller than the value obtained in the absence of cofilin. The smaller K_{SV_S} suggests that the surrounding of the ε-ATP transformed into a more compact form due to the binding of cofilin. This conformational transition effectively reduced the probability that the acrylamide can approach the fluorophore molecule.

The quenching of fluorescence from the actin bound ε-ATP with acrylamide was tested in the presence of profilin as well (Fig. 5 *A*). The Stern-Volmer plot of the data showed the same downward curving tendency as it was seen before (Fig. 5 *B*.). The concentration of the actin was adjusted to 5 μM whereas the profilin concentration was 20 μM. Considering that the affinity of yeast profilin for muscle actin is 2.9 μM (33) the contribution of the profilin free actin was ~15.5% (~0.8 μM). This amount of free actin could not been considered as negligible during the analysis of the data as it was possible before in the case of cofilin.

The fluorescence lifetime measurements helped us to test the K_{SV_D} associated with the actin bound ε-ATP. In these experiments the actin concentration was adjusted to 20 μM, and 20 μM profilin was added to the sample solution. In this situation the fraction of the profilin free actin was ~31% (~6 μM). The acrylamide concentration was changed in six steps up to 0.3 M. Although there were three different ε-ATP populations in the samples (free ε-ATP; actin bound ε-ATP; actin-profilin bound ε-ATP) the analysis of the results revealed only two lifetime components. The χ^2 value for the fits were in the range of 2 ± 0.3. The shorter lifetime component (τ_1) followed the same tendency as it was seen before in the case of the unbound ε-ATP fraction and changed from 25.7 ± 0.01 ns to 1.4 ± 0.07 ns during the experiments. The calculated K_{SV_D} value for this component was $57.8 \pm 4.6\ M^{-1}$. Based on these facts we attributed this fraction to the free ε-ATP in the solution. The longer lifetime component (τ_2) of the actin bound ε-ATP was 31.07 ns, and did not change significantly during the quenching experiments. The fluorescence lifetime measurements could not distinguish between the profilin bound and unbound ε-ATP actin monomers, which suggests that the fluorescence lifetime of the ε-ATP in the central groove of actin was not sensitive to the binding of profilin. These observations also showed that the change of the fluorescence signal from the actin bound ε-ATP was not affected by dynamic quenching processes. We concluded that the quencher molecule could not effectively collide with the fluorophore to change its lifetime in its protein bound formation.

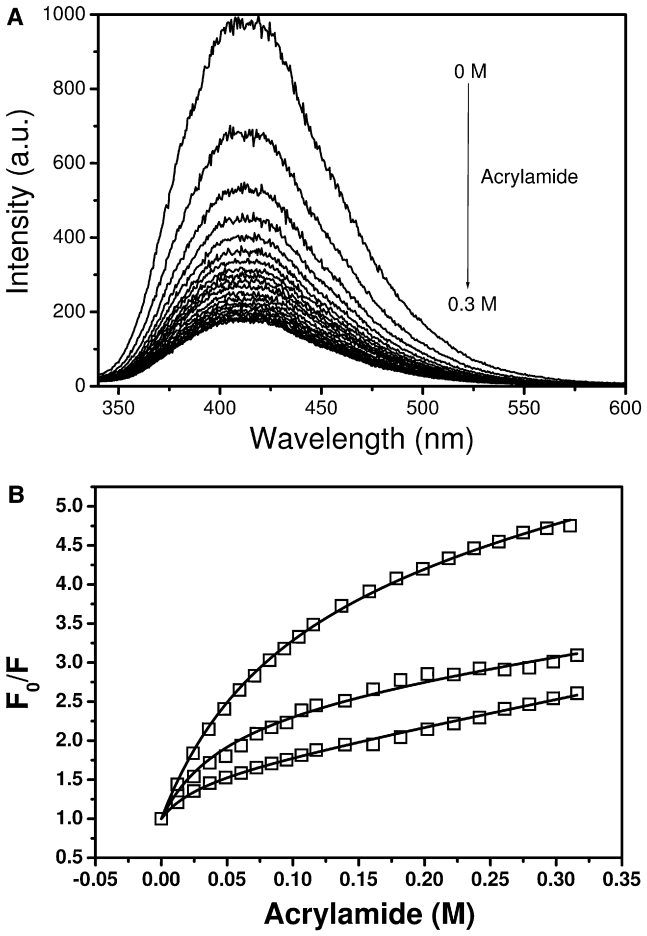

FIGURE 5 Quenching of the fluorescence of ε-ATP labeled actin monomers with acrylamide in the presence of profilin. (*A*) The change of the fluorescence spectrum of the ε-ATP labeled monomers (5 μM) in the presence of profilin (20 μM) with increasing acrylamide concentration (0–0.3 M). (*B*) The Stern-Volmer plots from the steady-state quenching experiments with 5 μM ε-ATP labeled actin monomers in the presence of 20 μM profilin (□) at different acrylamide concentrations (0–0.3 M). The calculated K_{SV_S} value for the actin bound ε-ATP was $3.5 \pm 1.5\ M^{-1}$ in the presence of the profilin.

It was possible to evaluate the involvement of static processes in the change of the steady-state fluorescence signal of the actin-bound ε-ATP by using the Eq. 4. The known parameters of $K_{SV\_S\_free-\varepsilon ATP}$ ($0\ M^{-1}$), $K_{SV\_D\_free-\varepsilon ATP}$ ($54.05\ M^{-1}$), and $K_{SV\_S\_bound-\varepsilon ATP}$ ($0.24\ M^{-1}$) were used as fixed parameters during the fitting procedure. The unknown parameters of the fractional contribution in the fluorescence signal (f) and the K_{SV_S} for the ε-ATP bound actin monomer were used as variables during the analysis of the data.

The result of the fitting procedure showed that the static quenching constant (K_{SV_S}) for the actin bound ε-ATP in the presence of profilin was $3.5 \pm 1.5\ M^{-1}$ ($n = 3$) (Fig. 5 *B*) and the fraction of the free ε-ATP varied in the range of 36–80%. The K_{SV_S} was higher than the result obtained in the absence of the profilin ($0.24 \pm 0.05\ M^{-1}$), which suggested that the ATP binding cleft became more accessible to the quenchers in the presence of the profilin molecule probably due to the opening of the nucleotide-binding cleft.

In summary the results of the quenching experiments showed that the actin bound ε-ATP could only be quenched through static quenching processes with a K_{SV_S} value of $0.24 \pm 0.05\ M^{-1}$ (Fig. 2 *B*). The presence of cofilin decreased this value to $0.034 \pm 0.017\ M^{-1}$ (Fig. 4 *B*) whereas the profilin had an opposite effect by increasing it to $3.5 \pm 1.5\ M^{-1}$ (Fig. 5 *B*).

CONCLUSIONS

Although a number of studies reported that the binding of actin-binding proteins could affect the rate of nucleotide exchange of the actin monomers, the relationship between the functional changes and the underlying conformational transitions is not clearly understood yet (42,43,66–68). It was shown that the nucleotide exchange rate in actin decreased in the presence of cofilin, whereas an increased rate was observed in the presence of profilin (9,13–15, 40,41,43). In accordance with these findings structural data suggested that the nucleotide-binding cleft of actin could open up in the presence of profilin, whereas the cofilin had an opposite effect on its structure (20,26,48). Despite the importance and the power of the structural methods in the understanding of protein functions, these methods have limitations in describing the details of the dynamic conformational changes in proteins due to certain restrictive ambient effects (e.g., crystal contacts, buffer conditions).

We described the intramolecular changes within the actin monomers by carrying out fluorescence quenching experiments. The advantage of this method is that it can provide information regarding the details of the conformational changes behind the functional differences under physiologically relevant conditions. The results showed that the accessibility of the nucleotide-binding cleft of actin decreased on cofilin binding, whereas an increased cleft accessibility was detected after the binding of profilin. These results are in good agreement with the observations from structural studies (20,26,48).

The conclusions from these quenching experiments also correlate well with the previously described effects of the actin-binding proteins on the functional properties of actin (9,13–15,40,41,43), which provides evidence that there is a direct correlation between the conformational state of actin and its functional properties.

Future work with other actin monomer binding proteins (e.g., thymosin-β_4 and various WH2 domain proteins) may lead us to a general conclusion concerning the relationship between the biochemical functions of actin monomer binding proteins and their effects on the structure of the nucleotide binding cleft of actin.

We are grateful to the late Professor Béla Somogyi for the support he produced at the beginning of this work.

This work was supported by grants from the Hungarian Scientific Research Fund (OTKA grant K60186 and K60968 to M.Ny.), the Hungarian National Office for Research and Technology (GVOP-3.2.1.-2004-04-0190/3.0 and GVOP-3.2.1.-2004-04-0228/3.0) and by the Academy of Finland and Sigrid Juselius Foundation (P.L.). Miklós Nyitrai holds a Wellcome Trust International Senior Research Fellowship in Biomedical Sciences.

REFERENCES

1. dos Remedios, C. G., D. Chhabra, M. Kekic, I. V. Dedova, M. Tsubakihara, et al. 2003. Actin binding proteins: regulation of cytoskeletal microfilaments. *Physiol. Rev.* 83:433–473.
2. Paavilainen, V. O., E. Bertling, S. Falck, and P. Lappalainen. 2004. Regulation of cytoskeletal dynamics by actin-monomer-binding proteins. *Trends Cell Biol.* 14:386–394.
3. Moon, A., and D. G. Drubin. 1995. The ADF/cofilin proteins: stimulus-responsive modulators of actin dynamics. *Mol. Biol. Cell.* 6:1423–1431.
4. Nishida, E., S. Maekawa, and H. Sakai. 1984. Cofilin, a protein in porcine brain that binds to actin filaments and inhibits their interactions with myosin and tropomyosin. *Biochemistry.* 23:5307–5313.
5. Theriot, J. A. 1997. Accelerating on a treadmill: ADF/cofilin promotes rapid actin filament turnover in the dynamic cytoskeleton. *J. Cell Biol.* 136:1165–1168.
6. Hotulainen, P., E. Paunola, M. K. Vartiainen, and P. Lappalainen. 2005. Actin-depolymerizing factor and cofilin-1 play overlapping roles in promoting rapid F-actin depolymerization in mammalian nonmuscle cells. *Mol. Biol. Cell.* 16:649–664.
7. Okreglak, V., and D. G. Drubin. 2007. Cofilin recruitment and function during actin-mediated endocytosis dictated by actin nucleotide state. *J. Cell Biol.* 178:1251–1264.
8. Carlier, M. F., V. Laurent, J. Santolini, R. Melki, D. Didry, et al. 1997. Actin depolymerizing factor (ADF/cofilin) enhances the rate of filament turnover: implication in actin-based motility. *J. Cell Biol.* 136:1307–1322.
9. Andrianantoandro, E., and T. D. Pollard. 2006. Mechanism of actin filament turnover by severing and nucleation at different concentrations of ADF/cofilin. *Mol. Cell.* 24:13–23.
10. Blanchoin, L., and T. D. Pollard. 1999. Mechanism of interaction of Acanthamoeba actophorin (ADF/Cofilin) with actin filaments. *J. Biol. Chem.* 274:15538–15546.
11. Maciver, S. K., and A. G. Weeds. 1994. Actophorin preferentially binds monomeric ADP-actin over ATP-bound actin: consequences for cell locomotion. *FEBS Lett.* 347:251–256.
12. Vartiainen, M. K., T. Mustonen, P. K. Mattila, P. J. Ojala, I. Thesleff, et al. 2002. The three mouse actin-depolymerizing factor/cofilins evolved to fulfill cell-type-specific requirements for actin dynamics. *Mol. Biol. Cell.* 13:183–194.
13. Bamburg, J. R. 1999. Proteins of the ADF/cofilin family: essential regulators of actin dynamics. *Annu. Rev. Cell Dev. Biol.* 15:185–230.
14. Lappalainen, P., E. V. Fedorov, A. A. Fedorov, S. C. Almo, and D. G. Drubin. 1997. Essential functions and actin-binding surfaces of yeast cofilin revealed by systematic mutagenesis. *EMBO J.* 16:5520–5530.
15. Nishida, E. 1985. Opposite effects of cofilin and profilin from porcine brain on rate of exchange of actin-bound adenosine 5′-triphosphate. *Biochemistry.* 24:1160–1164.
16. Blanchoin, L., and T. D. Pollard. 1998. Interaction of actin monomers with Acanthamoeba actophorin (ADF/cofilin) and profilin. *J. Biol. Chem.* 273:25106–25111.
17. Dominguez, R. 2004. Actin-binding proteins–a unifying hypothesis. *Trends Biochem. Sci.* 29:572–578.
18. Mannherz, H. G., E. Ballweber, M. Galla, S. Villard, C. Granier, et al. 2007. Mapping the ADF/cofilin binding site on monomeric actin by competitive cross-linking and peptide array: evidence for a second binding site on monomeric actin. *J. Mol. Biol.* 366:745–755.
19. Wriggers, W., J. X. Tang, T. Azuma, P. W. Marks, and P. A. Janmey. 1998. Cofilin and gelsolin segment-1: molecular dynamics simulation and biochemical analysis predict a similar actin binding mode. *J. Mol. Biol.* 282:921–932.
20. Paavilainen, V. O., E. Oksanen, A. Goldman, and P. Lappalainen. 2008. Structure of the actin-depolymerizing factor homology domain in complex with actin. *J. Cell Biol.* 182:51–59.
21. Goode, B. L., D. G. Drubin, and P. Lappalainen. 1998. Regulation of the cortical actin cytoskeleton in budding yeast by twinfilin, a ubiquitous actin monomer-sequestering protein. *J. Cell Biol.* 142:723–733.
22. Helfer, E., E. M. Nevalainen, P. Naumanen, S. Romero, D. Didry, et al. 2006. Mammalian twinfilin sequesters ADP-G-actin and caps filament barbed ends: implications in motility. *EMBO J.* 25:1184–1195.
23. Ojala, P. J., V. O. Paavilainen, M. K. Vartiainen, R. Tuma, A. G. Weeds, et al. 2002. The two ADF-H domains of twinfilin play functionally distinct roles in interactions with actin monomers. *Mol. Biol. Cell.* 13:3811–3821.
24. Paavilainen, V. O., M. Hellman, E. Helfer, M. Bovellan, A. Annila, et al. 2007. Structural basis and evolutionary origin of actin filament capping by twinfilin. *Proc. Natl. Acad. Sci. USA.* 104:3113–3118.
25. Page, R., U. Lindberg, and C. E. Schutt. 1998. Domain motions in actin. *J. Mol. Biol.* 280:463–474.
26. Chik, J. K., U. Lindberg, and C. E. Schutt. 1996. The structure of an open state of beta-actin at 2.65 A resolution. *J. Mol. Biol.* 263:607–623.
27. Bobkov, A. A., A. Muhlrad, D. A. Pavlov, K. Kokabi, A. Yilmaz, et al. 2006. Cooperative effects of cofilin (ADF) on actin structure suggest allosteric mechanism of cofilin function. *J. Mol. Biol.* 356: 325–334.
28. Kamal, J. K., S. A. Benchaar, K. Takamoto, E. Reisler, and M. R. Chance. 2007. Three-dimensional structure of cofilin bound to monomeric actin derived by structural mass spectrometry data. *Proc. Natl. Acad. Sci. USA.* 104:7910–7915.
29. Muhlrad, A., D. Pavlov, Y. M. Peyser, and E. Reisler. 2006. Inorganic phosphate regulates the binding of cofilin to actin filaments. *FEBS J.* 273:1488–1496.
30. Witke, W. 2004. The role of profilin complexes in cell motility and other cellular processes. *Trends Cell Biol.* 14:461–469.
31. Buss, F., C. Temm-Grove, S. Henning, and B. M. Jockusch. 1992. Distribution of profilin in fibroblasts correlates with the presence of highly dynamic actin filaments. *Cell Motil. Cytoskeleton.* 22:51–61.
32. Blanchoin, L., T. D. Pollard, and R. D. Mullins. 2000. Interactions of ADF/cofilin, Arp2/3 complex, capping protein and profilin in remodeling of branched actin filament networks. *Curr. Biol.* 10:1273–1282.
33. Eads, J. C., N. M. Mahoney, S. Vorobiev, A. R. Bresnick, K. K. Wen, et al. 1998. Structure determination and characterization of *Saccharomyces cerevisiae* profilin. *Biochemistry.* 37:11171–11181.
34. Lal, A. A., and E. D. Korn. 1985. Reinvestigation of the inhibition of actin polymerization by profilin. *J. Biol. Chem.* 260:10132–10138.
35. Pantaloni, D., and M. F. Carlier. 1993. How profilin promotes actin filament assembly in the presence of thymosin beta 4. *Cell.* 75:1007–1014.
36. Vinson, V. K., E. M. De La Cruz, H. N. Higgs, and T. D. Pollard. 1998. Interactions of Acanthamoeba profilin with actin and nucleotides bound to actin. *Biochemistry.* 37:10871–10880.
37. Ferron, F., G. Rebowski, S. H. Lee, and R. Dominguez. 2007. Structural basis for the recruitment of profilin-actin complexes during filament elongation by Ena/VASP. *EMBO J.* 26:4597–4606.
38. Perelroizen, I., D. Didry, H. Christensen, N. H. Chua, and M. F. Carlier. 1996. Role of nucleotide exchange and hydrolysis in the function of profilin in action assembly. *J. Biol. Chem.* 271:12302–12309.
39. Romero, S., C. Le Clainche, D. Didry, C. Egile, D. Pantaloni, et al. 2004. Formin is a processive motor that requires profilin to accelerate actin assembly and associated ATP hydrolysis. *Cell.* 119:419–429.
40. Goldschmidt-Clermont, P. J., L. M. Machesky, S. K. Doberstein, and T. D. Pollard. 1991. Mechanism of the interaction of human platelet profilin with actin. *J. Cell Biol.* 113:1081–1089.

41. Korenbaum, E., P. Nordberg, C. Bjorkegren-Sjogren, C. E. Schutt, U. Lindberg, et al. 1998. The role of profilin in actin polymerization and nucleotide exchange. *Biochemistry.* 37:9274–9283.

42. Perelroizen, I., M. F. Carlier, and D. Pantaloni. 1995. Binding of divalent cation and nucleotide to G-actin in the presence of profilin. *J. Biol. Chem.* 270:1501–1508.

43. Selden, L. A., H. J. Kinosian, J. E. Estes, and L. C. Gershman. 1999. Impact of profilin on actin-bound nucleotide exchange and actin polymerization dynamics. *Biochemistry.* 38:2769–2778.

44. Lassing, I., and U. Lindberg. 1985. Specific interaction between phosphatidylinositol 4,5-bisphosphate and profilactin. *Nature.* 314: 472–474.

45. Cedergren-Zeppezauer, E. S., N. C. Goonesekere, M. D. Rozycki, J. C. Myslik, Z. Dauter, et al. 1994. Crystallization and structure determination of bovine profilin at 2.0 A resolution. *J. Mol. Biol.* 240:459–475.

46. Fedorov, A. A., K. A. Magnus, M. H. Graupe, E. E. Lattman, T. D. Pollard, et al. 1994. X-ray structures of isoforms of the actin-binding protein profilin that differ in their affinity for phosphatidylinositol phosphates. *Proc. Natl. Acad. Sci. USA.* 91:8636–8640.

47. Metzler, W. J., B. T. Farmer 2nd, K. L. Constantine, M. S. Friedrichs, T. Lavoie, et al. 1995. Refined solution structure of human profilin I. *Protein Sci.* 4:450–459.

48. Schutt, C. E., J. C. Myslik, M. D. Rozycki, N. C. Goonesekere, and U. Lindberg. 1993. The structure of crystalline profilin-beta-actin. *Nature.* 365:810–816.

49. Baek, K., X. Liu, F. Ferron, S. Shu, E. D. Korn, et al. 2008. Modulation of actin structure and function by phosphorylation of Tyr-53 and profilin binding. *Proc. Natl. Acad. Sci. USA.* 105:11748–11753.

50. Minehardt, T. J., P. A. Kollman, R. Cooke, and E. Pate. 2006. The open nucleotide pocket of the profilin/actin x-ray structure is unstable and closes in the absence of profilin. *Biophys. J.* 90:2445–2449.

51. De La Cruz, E. M., E. M. Ostap, R. A. Brundage, K. S. Reddy, H. L. Sweeney, et al. 2000. Thymosin-beta(4) changes the conformation and dynamics of actin monomers. *Biophys. J.* 78:2516–2527.

52. Dedova, I. V., O. P. Nikolaeva, D. Safer, E. M. De La Cruz, and C. G. dos Remedios. 2006. Thymosin beta4 induces a conformational change in actin monomers. *Biophys. J.* 90:985–992.

53. Irobi, E., A. H. Aguda, M. Larsson, C. Guerin, H. L. Yin, et al. 2004. Structural basis of actin sequestration by thymosin-beta4: implications for WH2 proteins. *EMBO J.* 23:3599–3608.

54. Feuer, G., F. Molnár, E. Pettko, and F. B. Straub. 1948. Studies on the composition and polymerization of actin. *Hung. Acta Physiol.* 1: 150–163.

55. Mossakowska, M., J. Belagyi, and H. Strzelecka-Golaszewska. 1988. An EPR study of the rotational dynamics of actins from striated and smooth muscle and their complexes with heavy meromyosin. *Eur. J. Biochem.* 175:557–564.

56. Spudich, J. A., and S. Watt. 1971. The regulation of rabbit skeletal muscle contraction. I. Biochemical studies of the interaction of the tropomyosin-troponin complex with actin and the proteolytic fragments of myosin. *J. Biol. Chem.* 246:4866–4871.

57. Houk, T. W., Jr., and K. Ue. 1974. The measurement of actin concentration in solution: a comparison of methods. *Anal. Biochem.* 62:66–74.

58. Elzinga, M., J. H. Collins, W. M. Kuehl, and R. S. Adelstein. 1973. Complete amino-acid sequence of actin of rabbit skeletal muscle. *Proc. Natl. Acad. Sci. USA.* 70:2687–2691.

59. Lakowicz, J. R. 1983. Measurement of fluorescence lifetime. *In* Principles of Fluorescence Spectroscopy. Joseph R. Lakowicz, editor. Plenum Press, New York. 51–93.

60. Lakowicz, J. R. 1983. Quenching of fluorescence. *In* Principles of Fluorescence Spectroscopy. Joseph R. Lakowicz, editor. Plenum Press, New York. 257–301.

61. Ando, T., J. A. Duke, Y. Tonomura, and M. F. Morales. 1982. Spectroscopic isolation of ES complexes of myosin subfragment-1 ATPase by fluorescence quenching. *Biochem. Biophys. Res. Commun.* 109:1–6.

62. Harvey, S. C., and H. C. Cheung. 1976. Fluorescence studies of 1,N6-ethenoadenosine triphosphate bound to G-actin: the nucleotide base is inaccessible to water. *Biochem. Biophys. Res. Commun.* 73:865–868.

63. Root, D. D., and E. Reisler. 1992. The accessibility of etheno-nucleotides to collisional quenchers and the nucleotide cleft in G- and F-actin. *Protein Sci.* 1:1014–1022.

64. Rosenfeld, S. S., and E. W. Taylor. 1984. Reactions of 1–N6-ethenoadenosine nucleotides with myosin subfragment 1 and acto-subfragment 1 of skeletal and smooth muscle. *J. Biol. Chem.* 259:11920–11929.

65. Johnson, D. A., and J. Yguerabide. 1985. Solute accessibility to N epsilon-fluorescein isothiocyanate-lysine-23 cobra alpha-toxin bound to the acetylcholine receptor. A consideration of the effect of rotational diffusion and orientation constraints on fluorescence quenching. *Biophys. J.* 48:949–955.

66. Goldschmidt-Clermont, P. J., M. I. Furman, D. Wachsstock, D. Safer, V. T. Nachmias, et al. 1992. The control of actin nucleotide exchange by thymosin beta 4 and profilin. A potential regulatory mechanism for actin polymerization in cells. *Mol. Biol. Cell.* 3:1015–1024.

67. Hawkins, M., B. Pope, S. K. Maciver, and A. G. Weeds. 1993. Human actin depolymerizing factor mediates a pH-sensitive destruction of actin filaments. *Biochemistry.* 32:9985–9993.

68. Mockrin, S. C., and E. D. Korn. 1980. Acanthamoeba profilin interacts with G-actin to increase the rate of exchange of actin-bound adenosine 5′-triphosphate. *Biochemistry.* 19:5359–5362.